Friction Stir Welding Simulation in Abaqus/Explicit

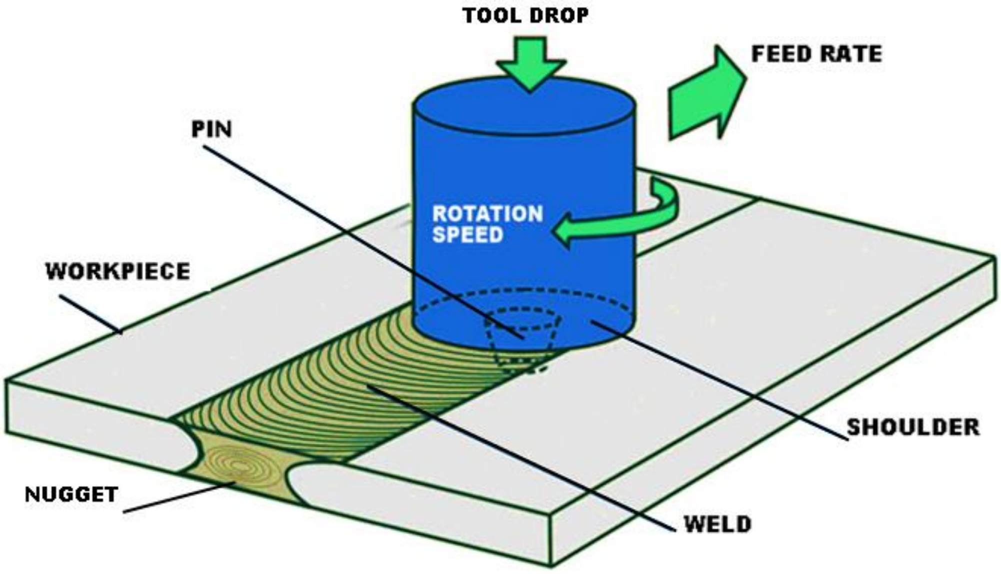

Image courtesy UQAC Friction Stir Welding Center

Version 1.0 - 10/11/2018
Written by: Alireza CHADEGANI
Validated by: David PALMER
Edited by: Arati DESAI

3DEXPERIENCE 2018x FP.1822

Executive Summary

Friction stir welding (FSW) technology involves joining metals without fusion or filler materials. Welded joints are created by the combination of frictional heating and permanent mechanical deformations.

By deploying an Abaqus/Explicit coupled thermal-stress analysis together with the coupled Eulerian-Lagrangian (CEL) formulation, we provide details and guidance for modeling a welded butt joint consisting of a ST4340-C30/AL6061-T6 matrix.

This document is intended for the engineers and analysts concerned with modeling the advanced joining technology in Abaqus/Explicit.

Contents

1. Introduction

Friction stir welding (FSW) is a solid-state joining method invented at The Welding Institute, Cambridge, UK, that involves joining metals without fusion or filler materials. It is commonly used in many critical applications for the joining of structural components made of aluminum. In particular, it is used to join high-strength aerospace aluminum alloys that are hard to weld by conventional fusion welding. FSW has been demonstrated to produce strong and ductile joints in systems that have proven difficult for conventional welding techniques. The process is most suitable for long, flat components such as plates and sheets but can be adapted for pipes, hollow sections, and positional welding. The welds are created by the combination of frictional heating and mechanical permanent deformation which are both induced by a rotating tool. This joining technique is energy efficient, environmentally friendly, and versatile.

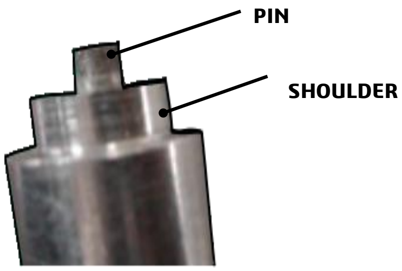

Figure 1: Friction stir welding tool [Ref. 1]

1.1. Friction Stir Welding Process

Even though the FSW process involves complex interactions between the material properties, material flow, heat transfer, and applied forces and boundary conditions, the operational principles are quite simple. The tool has a circular section except at the end pin where it has either a threaded or unthreaded surface; the junction between the cylindrical portion and the pin is known as the shoulder; see Figure 1.

The pin penetrates the workpieces along the butt joint, whereas the shoulder contacts the top flat surfaces of the workpiece. Heat is generated primarily by friction between the tool shoulder and the workpieces as the tool rotates and translates. The localized heating softens the material around the pin and the combination of tool rotation and translation leads to movement of material from the front of the pin to the back of the pin with respect to the direction of travel. A smaller, volumetric, contribution to heat generation also arises from the adiabatic heating from instantaneous deformation near the pin; see Figure 2.

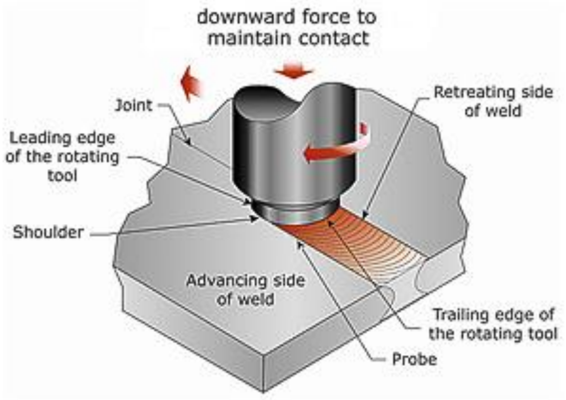

Figure 2: Schematic representation of friction stir welding process [Ref. 2]

To ensure that a sufficient heat input per unit length is provided for the FSW process, the welding parameters are typically adjusted so that the ratio of frictional heating to volumetric deformation is constant. Note that induced heating decreases as the workpiece thickness increases. The microstructure of friction-stir welded joints depends on the tool parameters (dimension and material), the rotation speed and feed rate, the applied pressure (via vertical force or displacement), and the characteristics of the material being joined.

1.2. Microstructure of Friction Stir Welded Joints

As shown in Figure 3 below, friction-stir welded joints consist of four zones presenting different microstructure and mechanical properties:

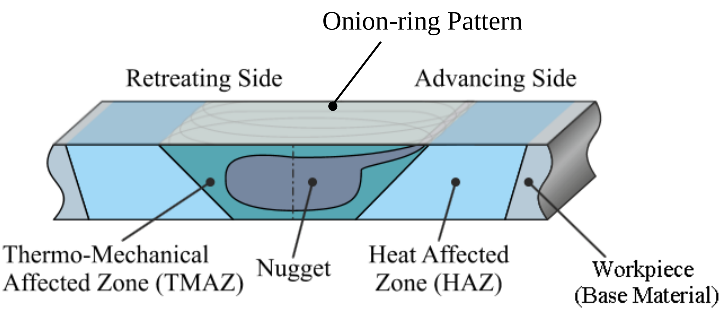

Figure 3: Schematic representation of friction-stir welded joints [Ref. 2]

• An inner central processing region called the "weld nugget" is strongly influenced by the shape of the pin and the shoulder as well as the thickness of the workpiece. This region is the most severely deformed and is dynamically recrystallized with micro grains.

• The thermomechanical affected zone (TMAZ) is subjected to intense plastic deformation and surrounds the nugget. In this region, the material is not mixed and there is no dynamic recrystallization, but the grains are deformed. The "onion-ring" pattern develops over the nugget and TMAZ.

• The heat affected zone (HAZ) is not subjected to plastic deformation (or strain hardening) and the microstructures are dependent upon the time-dependent process parameters (i.e., strain rate).

• The remaining portion of the workpiece consisting of the base material is in a quasi-equilibrium thermal condition and does not experience large temperature change.

2. Computational Approach

There has been considerable effort to understand the various aspects of the FSW process, to study the effect of the FSW process parameters, and to classify the mechanical properties of welded joints; however, there are still many challenges to setting up accurate experiments. Thus, the finite element (FE) simulation method has been employed to better understand the complexities and reduce the cost of the FSW process.

Due to the presence of extreme material deformation during FSW, severe mesh distortions preclude the robust use of the conventional Lagrangian approach in which the mesh deforms directly with the material.

The coupled Eulerian-Lagrangian (CEL) [Ref. 3] and the Arbitrary Lagrangian–Eulerian (ALE) [Ref. 4] methods are among the advanced technologies available in Abaqus suitable for the modeling of extreme deformation. In contrast to the traditional Lagrangian formulation, the Eulerian mesh in the CEL approach acts as a stationary background grid through which the material flows.

Simulation of material flow and spatial temperature distribution can be achieved by the Eulerian formulation available in CEL; it is therefore chosen for the FSW modeling task.

The CEL technique in Abaqus combines both the Lagrangian and Eulerian approaches in the same analysis. This method enables you to selectively employ the Eulerian approach for bodies undergoing large (or extreme) deformations while the remaining bodies can be modeled using the conventional Lagrangian approach. The interaction between bodies is captured by the general contact capability, which automatically accounts for the contact of bodies modeled with either the Lagrangian or Eulerian approaches.

2.1. Finite Element Modeling Framework

We develop a CEL-based analysis in Abaqus/Explicit to study the FSW of ST4340-C30/AL6061-T6 matrix subjected to a tungsten carbide (WC) tool. In this paper, we investigate the weld zone development, material flow, and spatial temperature distribution.

Fully coupled thermal-stress analysis is used to account for heat generated by frictional contact at the interface of the tool and the workpiece as well as the generation of heat by plastic deformation. The material temperature rises sufficiently high to affect the mechanical response (or microstructure) of the material. Note that for this analysis type, temperature is an active degree of freedom. Hence, a fully coupled thermal-stress analysis is invoked with the keyword:

```
*DYNAMIC TEMPERATURE-DISPLACEMENT, EXPLICIT
```

2.1.1. Eulerian Workpiece

The workpiece (350mm x 210mm x 2.25mm) is defined as Eulerian and the tool is defined as Lagrangian. The Eulerian domain is meshed using 8-node thermally-coupled linear multi-material, reduced integration brick (or solid) elements with default viscous hourglass control (EC3D8RT). Approximately 848k elements were used to discretize the workpiece.

The workpiece is horizontally divided into two equal sections where the volume fractions of ST4340-C30 and AL6061-T6 are assigned to the corresponding element sets (named ST_HORZ and AL_HORZ). This allows the single continuous Eulerian mesh to represent the separate material instances as shown in Figure 4. Note that an extra 0.75 mm-thick layer of Eulerian domain above the workpiece top surface is included as a void space and the corresponding volume fraction of material is set to zero. The void region allows us to capture the ejection of material during the initial tool drop and first contact and also later during the FSW process. The initial volume fractions are assigned as:

```
*INITIAL CONDITIONS, TYPE=VOLUME FRACTION
 AL_HORZ, AL, 1.0
 ST_HORZ, ST, 1.0
```

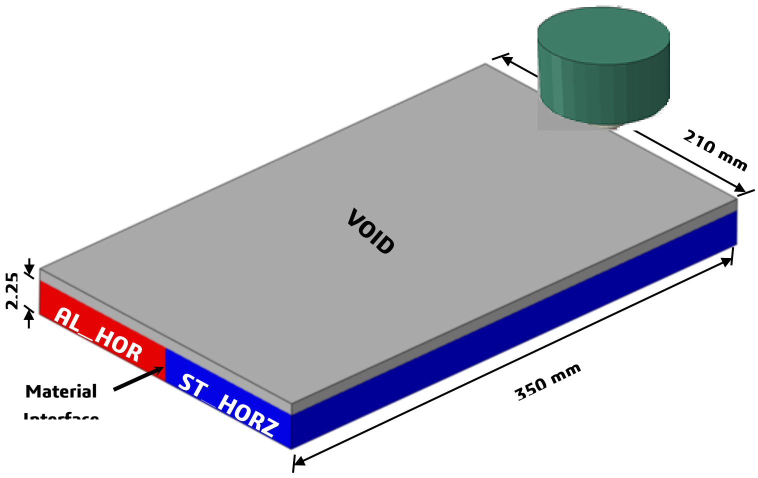

Figure 4: Geometry, dimensions and material assignment in workpiece

We assume that material is not allowed to enter or leave the Eulerian domain through a surface intersecting the plane at the point where the tool is initially located. However, material can exit the domain through all other surfaces. This condition is specified as:

```
*EULERIAN BOUNDARY, INFLOW=NONE, OUTFLOW=FREE
```

2.1.2. Lagrangian Tool

The cylindrical tool shown in Figure 5 below, has a smooth (or unthreaded) pin and is discretized into approximately 1.7k 8-node thermally coupled reduced integration brick elements using the default relaxed stiffness hourglass control (C3D8RT). The tool's rotational axis is tilted forward (i.e., in the direction of travel) by 2 degrees. We assume the tool to be rigid, since it experiences considerably less deformation than the workpiece. The rigid constraint is defined as:

```
*RIGID BODY, REFNODE=RB_TL, ELSET=TL, POSITION=CENTER OF MASS
```

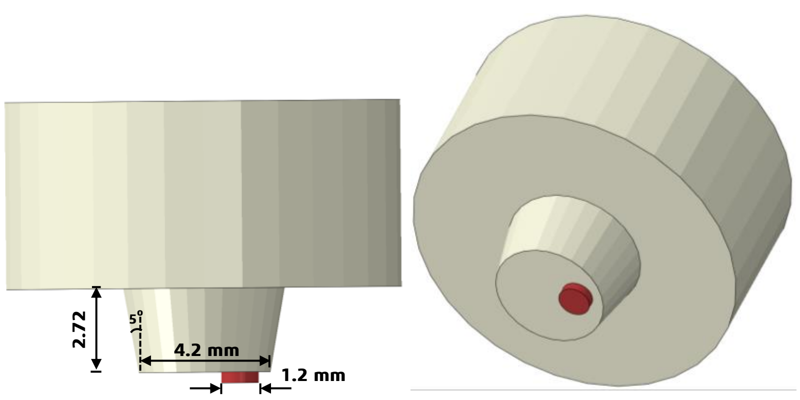

Figure 5: Schematic representation of tool

2.1.3. Contact Interaction Between Tool and Workpiece

General contact is used to model the contact interactions between the tool and the workpiece. The only heat sources here are friction at the workpiece-tool interface and plastic deformations. Therefore, as the normal and tangential contact forces are being generated, the resulting frictional heat will diffuse into the material points of the workpiece mesh.

To capture contact between bodies modeled as Lagrangian and Eulerian, Abaqus/Explicit utilizes an enhanced immersed boundary method [Ref. 6] that allows the material interfaces to be examined accurately. Eulerian-to-Eulerian contact is considered by default in an analysis involving Eulerian domains. Note that when the necessary contact between the parts of the rigid tool is excluded, the contact domain is specified with the following keywords:

```
*CONTACT
*CONTACT INCLUSIONS, ALL EXTERIOR
*CONTACT EXCLUSIONS
*CONTACT PROPERTY ASSIGNMENT
```

The general contact algorithm uses the penalty method to enforce the normal contact constraint, and Coulomb friction with a coefficient of 0.8 is specified. We assume that all of the energy generated by friction at the interface is dissipated as heat evenly between the two interacting surfaces. The surface interaction properties are specified with:

```
*SURFACE INTERACTION, NAME=FRIC
*FRICTION
*GAP HEAT GENERATION
```

2.1.4. Plastic Dissipation and Heating in Workpiece

As described earlier, the only sources of heat are frictional sliding and plastic deformation. We assume that 90% of the energy spent in plastic deformation is dissipated as heat. In addition to heat being conducted between the tool and workpiece, heat is also diffused within the workpiece. Thermal expansion is also included in the material definitions. These features are included with the following keywords:

```
*CONDUCTIVITY
*SPECIFIC HEAT
*EXPANSION
*INELASTIC HEAT FRACTION
```

2.1.5. Initial and Boundary Conditions

We hold (or fix) the bottom surface of the workpiece stationary in all directions. Hence, as the tool sweeps along the interface to form the weld, the materials flow as they come into contact with the moving tool. The Tool is initially at rest so that all rotational and translation components of the velocity are assumed to be zero. Boundary conditions are specified as:

```
*BOUNDARY, TYPE=VELOCITY
```

In addition, the initial temperature is set to 25°C (293.15K) for the Eulerian material instance:

```
*INITIAL CONDITIONS, TYPE=TEMPERATURE
 AL_HORZ, 293.15
 ST_HORZ, 293.15
```

2.1.6. Material Models

Workpiece Material Properties

In the present study, the material considered for the workpiece is ST4340-C30/AL6061-T6 matrix. We assume that the material is isotropic; in the plastic regime the hardening is assumed to be a function of strain and strain-rate. The material also experiences temperature softening.

The nature of the FSW process is to induce high strain rate deformations; we have therefore chosen the Johnson-Cook material model [Ref. 7] for this application. The associated keywords are:

```
*PLASTIC, HARDENING=JOHNSON COOK
*RATE DEPENDENT, TYPE=JOHNSON COOK
```

The material parameters for the virgin ST4340-C30 and AL6061-T6 materials are presented in Tables 1-4.

Table 1. Material parameters for ST4340-C30.

Density (kg/m^3)	Young's Modulus (GPa)	Coefficient of Thermal Expansion (1/K)	Specific Heat (J/kg.K)	Thermal Conductivity (W/m.K)	Poisson's Ratio
7870.0	200.0	1.40e-5	481.0	50.0	0.30

Table 2. Parameters of Johnson-Cook material model for ST4340-C30.

A (MPa)	B (MPa)	n	m	C	$\theta_{melting}$ (K)
792.0	510.0	0.26	1.03	0.14	1793.0

Table 3. Material parameters for AL6061-T6.

Density (kg/m^3)	Young's Modulus (GPa)	Coefficient of Thermal Expansion (1/K)	Specific Heat (J/kg.K)	Thermal Conductivity (W/m.K)	Poisson's Ratio
2690.0	69.0	2.40e-5	888.0	180.	0.29

Table 4. Parameters of Johnson-Cook material model for AL6061-T6.

A (MPa)	B (MPa)	n	m	C	$\theta_{melting}$ (K)
324.0	114.0	0.42	1.34	0.002	925.0

Tool Material Properties

Abrasive/cutting tools used in FSW process are typically made from high-speed steel (HSS) or tungsten carbide (WC). These materials have very high strength and can endure working at high temperatures. Therefore, the tool is expected to undergo significantly less deformation than the workpiece and is declared rigid.

In the present study, the tool is treated as a linear elastic material. Material parameters are provided in Table 5.

Table 5. Material parameters for WC Tool.

Density (kg/m^3)	Young's Modulus (GPa)	Coefficient of Thermal Expansion (1/K)	Specific Heat (J/kg.K)	Thermal Conductivity (W/m.K)	Poisson's Ratio
15,300.0	411.0	4.5E-06	134.0	163.3	0.28

Wearing or Abrasion of the Workpiece

In the localized regions for which material points of the workpiece experience significant plastic deformation, damage (or failure) due to wearing (or abrasion) are considered to be the dominant energy-absorbing failure mode. Hence, we use the Johnson-Cook dynamic (or shear) failure model [Ref. 7] and list the damage parameters for ST4340-C30 and AL6061-T6, respectively, in Tables 6-7.

```
*DAMAGE INITIATION, CRITERION=JOHNSON COOK
```

Table 6. Parameters of Johnson-Cook dynamic failure model for ST4340-C30.

d_1	d_2	d_3	d_4	d_5
0.05	3.44	2.12	0.002	0.61

Table 7. Parameters of Johnson-Cook dynamic failure model for AL6061-T6.

d_1	d_2	d_3	d_4	d_5
0.77	1.45	0.47	0.0	1.60

2.1.7. Step Definitions and Loading Conditions

Three analysis steps are defined:

Step 1: The tool is dropped from an initial distance of 0.75 mm above the workpiece and during the first 0.35ms is brought onto the workpiece surface with an applied translational velocity of 0.02 mm/ms. The tool also achieves a steady-state revolution with an applied rotational velocity=90.0 rad/ms.

Step 2: The tool starts to sweep at a constant horizontal translational velocity along the interface of the ST4340-C30 and AL6061-T6 regions to join the materials together and create a weld.

Step 3: The tool is raised vertically from the surface of the joined workpiece.

We note that the step definitions could have been combined into a single step by defining appropriate total time amplitude curves [Ref. 8]. However, this simulation more closely mimics the actual manufacturing process by keeping three distinct steps.

2.1.8. Heat Transfer Model

We also specify surface-based convection [Ref. 9] of heat between the free surfaces of the workpiece and the ambient surroundings. We therefore define two film coefficients, for heat removal from (a) the bottom surface interacting with unforced air and (b) the top surface interacting with a water soluble cutting fluid (or coolant). Use the following keyword:

```
*SFILM
```

2.1.9. Mass Scaling and Stable Time Increment

Since the FSW process is quasi-static, we scale the rate of loading by scaling the mass of the tool. An appropriate level of mass scaling improves the computational efficiency while preserving the necessary degree of accuracy required for this class of problems [Ref. 10]. The mass scaling is specified as:

```
*VARIABLE MASS SCALING, DT=5E-06, TYPE=BELOW, FREQ=10, ELSET=TOOL
```

Here, we also take advantage of a conservative method to estimate the element stable time increment in Step 2. In addition, the element-by-element stable time incrementation method is used to reduce the chance of numerical difficulties that may arise due to excessive deformations of the workpiece materials. These options are specified on the main procedure definition keyword:

```
*DYNAMIC TEMPERATURE-DISPLACEMENT, EXPLICIT,
IMPROVED DT METHOD=NO, ELEMENT BY ELEMENT
```

3. Solution Diagnostics, Results, and Discussion

In this section, we discuss the possible issues that may come up during both the preprocessing and solution phases of the analysis. Later in this section, methods to generate results and recommendations to interpret correctness of the results are provided.

3.1. Diagnostics: Possible Issues during Analysis

Here, we list possible issues that may arise during the analysis.

Solver errors sometimes occur during CEL analysis and diagnostic messages are issued to help the user. Some examples:

- ***ERROR: There are a total of *n* excessively distorted elements.
- ***ERROR: The ratio of deformation speed in element *n* vs. the wave speed of the element, *f* exceeds the warning ratio.
- ***ERROR: The incremental strain in element *n* is *f*, which exceeds the warning ratio
- ***ERROR: Excessive rotation increment at node *i*.

The messages shown above are written to the status (.sta) file. Some model features to check include:

- The rate of loading may be too high; therefore, prescribe a rise time for the loading curve or reduce the rate of loading and prolong the total step time.
- The mass scaling may be too high.
- The stable time increment may be too large and more conservative incrementation is needed. Include the SCALE FACTOR keyword option on *DYNAMIC TEMPERATURE-DISPLACEMENT to scale the stable time increment.
- The Eulerian mesh may be too coarse.
- Penetration (or leakage) of Eulerian material into the Lagrangian domain usually occurs when the default penalty contact computed internally is not sufficient to enforce the normal component of the contact .
    - A remedy to this problem is to add fillets to sharp edges of the Lagrangian domain that are in contact with the Eulerian domain. Another recommendation is to refine the mesh in the Eulerian domain or activate adaptive mesh refinement in the Eulerian domain for the elements that are in contact with Lagrangian bodies with the CONT refinement criterion [Ref. 11].

```
*ADAPTIVE MESH REFINEMENT
 CONT, ALL
```

Note that both of these approaches may be needed to resolve leakage issues.

To ensure the correctness of the solution, consider these points when examining results:

- Strain (or internal) energy (ALLSE, ALLIE) should be always positive.
- The total energy balance (ETOTAL) should be within a physical range; i.e., no external (or additional) energy should be introduced in the analysis. This is to guarantee satisfaction of the 2nd law of thermodynamics.
- When mass scaling is used in a quasi-static simulation, kinetic energy should be less than 5% of the internal energy.
- When mass scaling is used, the Percent Change of Mass reported in the status file should be within a reasonable range.
- Work done by the mass scaling (ALLMW) should be less than the external work done by the prescribed loads and boundary conditions.
- Energy dissipated due to damping (ALLVD), such as bulk viscosity and numerical damping, as well as artificial strain energy (ALLAE), should be small in comparison with the internal (or strain) energy. A preferable ratio is less than 5%.

3.2. Results and Discussion

For the first and second steps, we assume downward vertical and horizontal translational velocities of the tool to be 8.0 and 0.02 mm/s, respectively. The rotational velocity of the tool about its axis of revolution is set to 90.0 rad/s.

When viewing the results in Abaqus/Viewer, we exclude the portion of the Eulerian domain with a void volume fraction; i.e., Isosurface variable EVF_VOID is set to 0.5 within the View Cut Manager.

As shown in Figures 6 (a) and (b) below, almost 99% of the deformation in the workpiece material is plastic. In addition, energies dissipated due to damping (ALLVD) and hourglass control (ALLAE) are negligible compared to the internal (ALLIE) energy. Note that the total energy (ETOTAL) decreases by about 10%, which is due to loss of workpiece material as it is ejected from the unbounded Eulerian domains. In addition, damage (or failure) due to wearing (or abrasion) in the workpiece is an energy-absorbing component contributing to the decrease in ETOTAL.

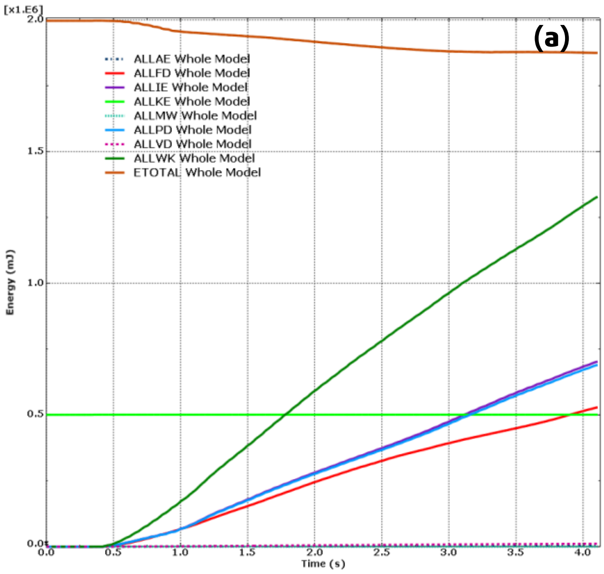

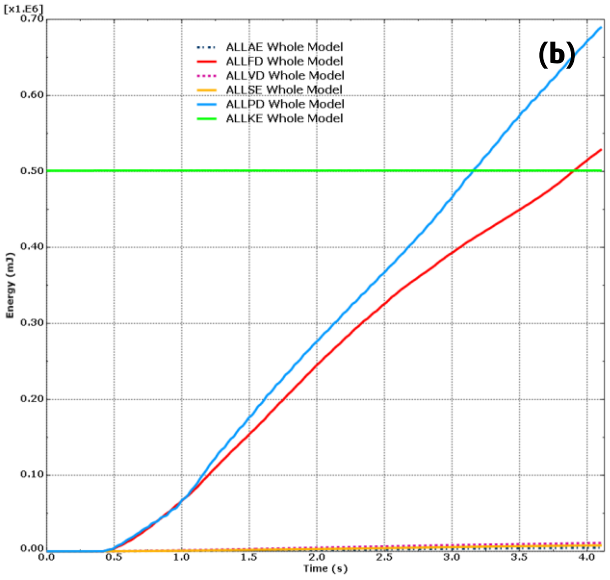

Figure 6: Time history of the components of the energy balance

The time history of the reaction forces and moments are shown in Figures 7 (a) and (b). The data is filtered in Abaqus/Viewer to eliminate the unnecessary high frequency noise. Note that the filtering could also be specified in the preprocessing phase within Abaqus/CAE; in this approach the filtered results are computed in the solver and written directly to the output database. The filter specification in Abaqus/Viewer is:

butterworthFilter (xyData = , cutoffFrequency = 5)

The tool in-plane reaction forces, RF1 and RF3 are similar in nature and magnitude and characterize the tool restraint forces in the lateral *x*- and z-directions as it sweeps through the workpiece in the 2nd step (starting at about 0.35 s). The vertical reaction force RF2 reflects the upward forces applied to the tool as it makes contact with the workpiece. There is a jump in reaction moment RM3 in Step 1 which is due to the rigid body motion of the tool. The reaction moments settle to a relatively constant rate as the tool sweeps the workpiece during Step 2.

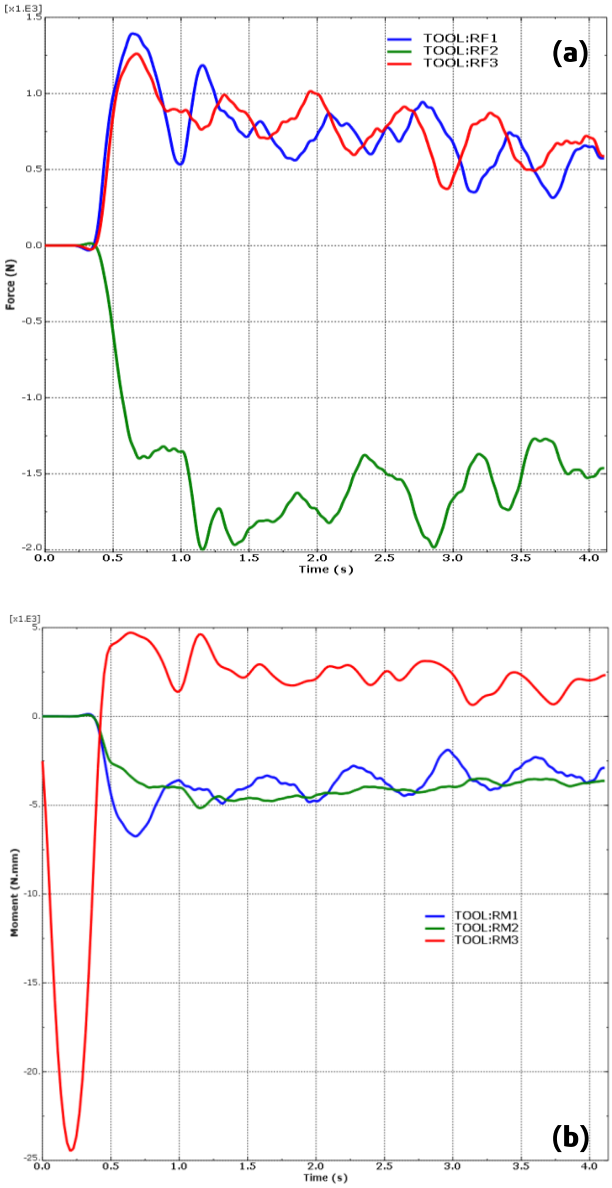

Figure 7: Time history of reaction forces and moments at the reference point of the Tool

The Figures 8 (a) - (c) below, display contour plots of temperature at 0.27, 0.27, and 0.36 s. The initiation and progression of a hot spot with an average temperature close to 550K, as well as the TMAZ and HAZ can be seen from these figures.

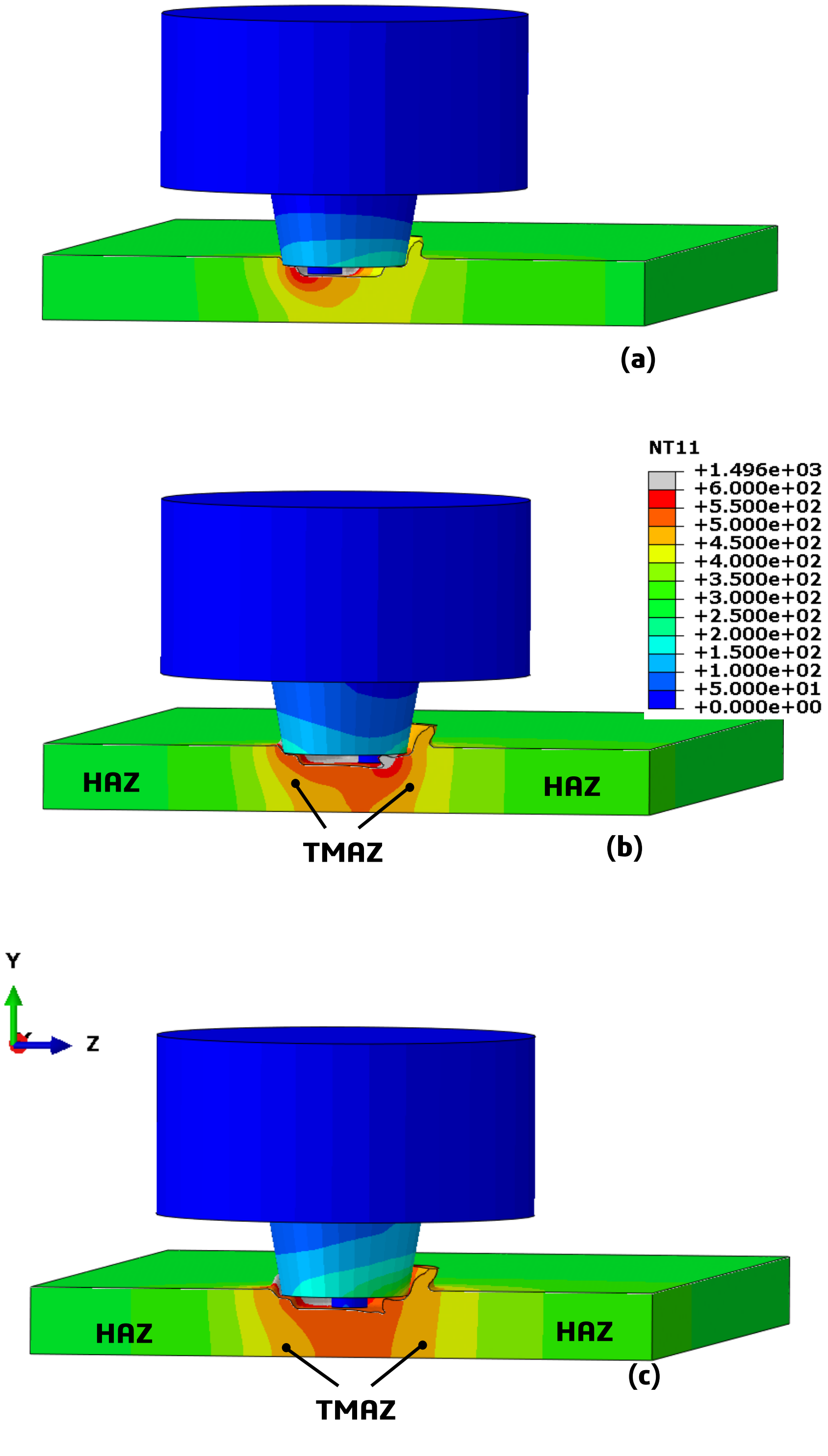

Figure 8: Formation of the weld-nugget zone (WNZ), TMAZ and HAZ

While the tool is sweeping the workpiece, an onion-ring pattern following the trailing edge of the tool is formed; see Figure 9 (a). This pattern encompasses a zone involving high stress (or strain) with the material instances developing a permanent butt joint. The pattern produced by Abaqus qualitatively compares well with a general pattern reported in the literature [Ref. 12] for an AL6061-T6/dissimilar metal joint; Figure 9 (b).

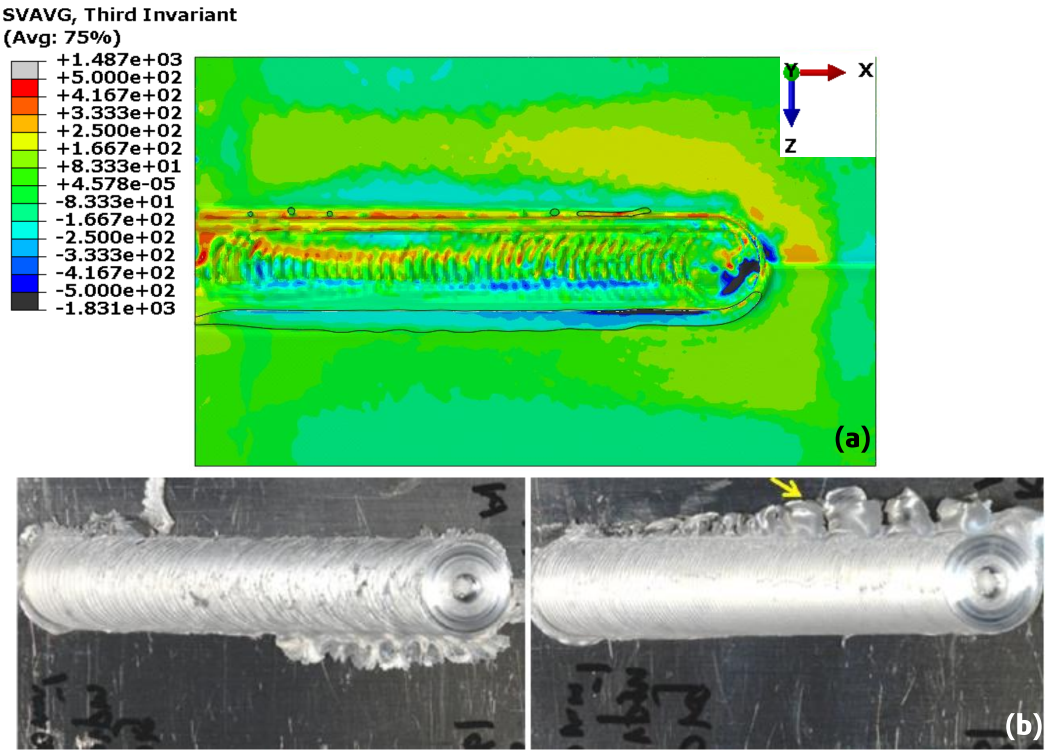

Figure 9: Onion-ring flow pattern in the workpiece compared with that given in Ref. 12

Figures 10 (a) and (b) show the volume fraction of the material instances after the butt joint is formed. Since ST4340-C30 is stiffer than AL6061-T6 and its melting temperature is almost double of that of AL6061-T6, the AL6061-T6 tends to be more involved in the FSW process and is easily diffused into ST4340-C30 after they have reached their melting temperatures. It is obvious from the figure that the trailing region, including the onion-ring pattern, has a higher strain energy release rate when it is subjected to a loading condition.

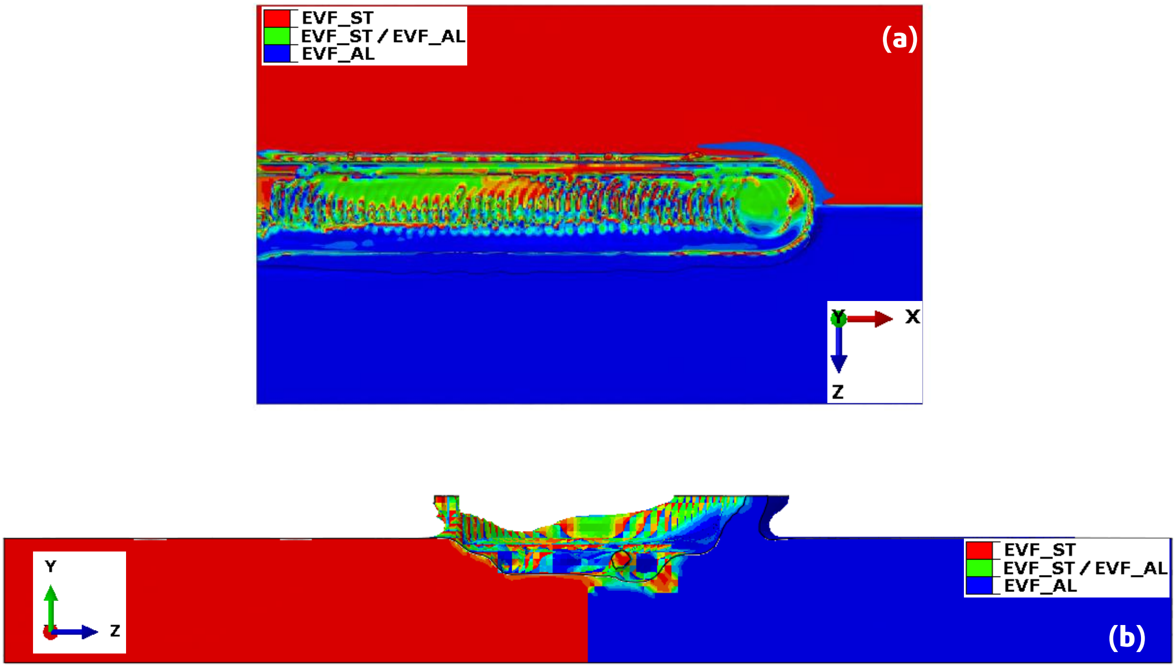

Figure 10: Distribution of material volume fraction produced by the FSW

4. References

1. http://www.uqac.ca/ceeuqac/index/csfm_english
2. http://www.niagarathermal.com/friction-stir-welding.html
3. Simulia User Assistance: Abaqus | Analysis | Analysis Techniques | Eulerian Analysis Techniques
4. Simulia User Assistance: Abaqus | Analysis | Analysis Techniques | Adaptivity Techniques | ALE adaptive meshing
5. Simulia User Assistance: Abaqus | Analysis | Analysis Techniques | Eulerian Analysis Techniques | Eulerian analysis
6. Lecture notes: Modeling Extreme Deformation and Fluid Flow with Abaqus
7. Simulia User Assistance: Abaqus | Materials | Inelastic Mechanical Properties | Metal plasticity | Johnson-Cook plasticity
8. Simulia User Assistance: Abaqus | Prescribed Conditions | Amplitude Curves
9. Simulia User Assistance: Abaqus | Prescribed Conditions | Loads | Thermal loads
10. Simulia User Assistance: Abaqus | Analysis | Analysis Techniques | Special-Purpose Techniques | Mass scaling
11. Simulia User Assistance: Abaqus | Analysis | Analysis Techniques | Eulerian Analysis Techniques | Defining adaptive mesh refinement in the Eulerian domain
12. Sun Y, Tsuji N., and Fujii H., Microstructure and Mechanical Properties of Dissimilar Friction Stir Welding between Ultrafine Grained 1050 and 6061-T6 Aluminum Alloys, *Metals* 2016, *6*(10), 249:5-12.

5. Document History

Document Revision	Date	Revised By	Changes/Notes
V1.0	10/11/2018	Alireza CHADEGANI	Original